Molecular Interaction of Water Vapor and Oxygen

Russell G. Wylie* and Robert S. Fisher

CSIRO Division of Applied Physics, National Measurement Laboratory, Lindfield, Australia 2070

The factor $f_w(T,p)$ by which oxygen increases the saturation vapor pressure of water has been measured accurately for temperatures of 25, 50, and 75 °C and pressures to 14 MPa. This paper outlines the measurements and describes their analysis to give the interaction second virial coefficient $B_{ow}(T)$ and the interaction third virial coefficient $C_{oow}(T)$ of the vapor−gas mixture. Because the work largely parallels the authors' work for water in air, already reported in detail, the present paper is relatively brief. Fitting Lennard-Jones potentials to the values of $B_{ow}(T)$ for the three temperatures shows the values to be highly mutually consistent and allows this coefficient and its derivatives to be calculated over a wide temperature range. The three values of $C_{oow}(T)$ define the magnitude of this quantity well for temperatures from about 0 to 100 °C, but for lack of a reliable theory of the form of its temperature dependence yield little information concerning its derivatives. No earlier published measurements or theoretical values of the coefficients appear to exist. The work allows the vapor-pressure enhancement factor $f_w(T,p)$ to be calculated for a wide range of conditions and provides a basis for the calculation of the thermodynamic properties of the water−oxygen system.

Introduction

The effect of oxygen on the concentration of water vapor in equilibrium with liquid water or ice is a little less than that of air. For example, for 20 °C and a pressure of 15 MPa the approximate effect of the intermolecular forces in the gas phase is an increase of 34% (for air, 39%), that of the pressure acting on the liquid phase (the Poynting effect) an increase of 12% (12%), and that of the oxygen dissolved in the liquid (the Raoult effect) a decrease of 0.3% (0.2%). The net effect is an increase of approximately 49% (55%).

As for water in air (Wylie and Fisher, 1996), we define the vapor-concentration enhancement factor $g_w(T,p)$ by

$$c_w = g_w(T,p)c_w^o \tag{1}$$

where c_w is the saturation concentration in moles per unit volume of water vapor in oxygen at the temperature T and total pressure p and c_w^o that of the pure vapor at the same temperature. Remembering that the partial pressure p_w of the vapor is the product of the vapor mole fraction x_w and the total pressure, we also define a vapor-pressure enhancement factor $f_w(T,p)$ by

$$p_w = f_w(T,p)p_w^o \tag{2}$$

where p_w^o is the saturation vapor pressure of pure water at T. Equation 2 is equivalent to

$$x_w = f_w p_w^o/p \tag{3}$$

It is easily shown that

$$f_w = (Z/Z_w^o)g_w \tag{4}$$

where Z_w^o is the compressibility factor of the pure saturated vapor and Z that of the saturated mixture.

Because of their close similarity to those detailed for water in air in our earlier paper (Wylie and Fisher, 1996), the theory, the method of measuring f_w, and the procedure for analyzing the experimental results need only be outlined here. However, some of the property data needed for the analysis require detailed consideration.

Throughout the paper the term "uncertainty", unless qualified, means the 3σ value obtained by summing the squares of its random and systematic parts. In the terminology developed by the International Organization for Standardization (ISO), the uncertainties quoted are *expanded uncertainties* obtained by multiplying the appropriately estimated standard deviations by a *coverage factor* of 3.

Outline of the Theory

To obtain the equation for ln f_w, the thermodynamic potential of the water in the gas mixture is equated to that of the water in the liquid phase. The corresponding equation for pure water vapor in equilibrium with liquid water is then subtracted. The required expression for the thermodynamic potential of the water in the gas is derived using the virial form of the equation of state of the mixture as this has an exact statistical-thermodynamic basis. This equation is

$$p\tilde{V}/RT = 1 + (B_{oo}x_o^2 + 2B_{ow}x_ox_w + B_{ww}x_w^2)/\tilde{V} + (C_{ooo}x_o^3 + 3C_{oow}x_o^2x_w + 3C_{oww}x_ox_w^2 + C_{www}x_w^3)/\tilde{V}^2 + \ldots \tag{5}$$

where $x_o = 1 - x_w$ is the mole fraction of oxygen, $\tilde{V}$ is the molar volume of the mixture, B_{oo} and B_{ww} are the second virial coefficients of, respectively, oxygen and water vapor, C_{ooo} and C_{www} are the corresponding third virial coefficients, and B_{ow}, C_{oow}, and C_{oww} are interaction virial coefficients. B_{ow} represents the interaction of a single oxygen molecule with a single water molecule, C_{oow} the interaction of two oxygen molecules with a single water molecule, and C_{oww} the interaction of a single oxygen molecule with two water molecules.

When expressions for the terms representing the Poynting and Raoult effects are obtained from simple thermodynamic formulas, the equation for ln f_w is found to be

0021-9568/96/1741-0175$12.00/0

$$\ln f_w = \ln(Z/Z_w^o) - (W - W^o) + (1/RT)\int_{p_w^o}^{p} \tilde{V}_w^{l,o}\,dp - x_o^l \quad (6)$$

where R is the molar gas constant, $\tilde{V}_w^{l,o}$ is the molar volume of pure liquid water, and x_o^l is the mole fraction of dissolved oxygen in the liquid, and where

$$W = 2\frac{\beta}{\tilde{V}} + \frac{3}{2}\frac{\gamma}{\tilde{V}^2} + \frac{4}{3}\frac{\delta}{\tilde{V}^3} + \ldots \quad (7)$$

in which

$$\beta = \beta_{ow}x_o + B_{ww}x_w$$

$$\gamma = C_{oow}x_o^2 + 2C_{oww}x_ox_w + C_{www}x_w^2$$

$$\delta = D_{ooow}x_o^3 + 3D_{oow}x_o^2x_w + 3D_{owww}x_ox_w^2 + D_{wwww}x_w^3 \quad (8)$$

and so on. To obtain W^o, we simply take $x_o = 0$ in eq 8. In view of eq 4, the expression for ln g_w is just the right-hand side of eq 6 with the first term deleted.

As f_w is involved in the calculation of x_w (eq 3) which in turn is involved in the calculation of $\tilde{V}$ and Z, the right-hand side of eq 6 has a small implicit dependence on f_w. Therefore, to calculate f_w from the equation when all the property values are known, an iteration procedure is appropriate. The sensitivites of the calculated f_w to changes in the values substituted for B_{ow}, C_{oow}, and C_{oww} are numerically not very different from the corresponding sensitivities for water in air illustrated in Figure 1 of Wylie and Fisher (1996). The use of eq 6 to derive data for $B_{ow}(T)$ and $C_{oow}(T)$ from measurements of $f_w(T,p)$ when the other physical properties are known is outlined below.

Measurements

Brief Outline of the Method. The measurements of f_w were made using the same apparatus as employed for water in air (Wylie and Fisher, 1996). Essentially, a flow of oxygen from high-pressure gas cylinders is reduced in pressure to the desired value and passed through a two-stage saturator in a temperature-controlled bath. The vapor−gas mixture is then further reduced to a convenient pressure of approximately 1400 kPa and passed through a train of cells in which the water is extracted chemically for weighing. The then dry gas is collected in a light-weight pressure vessel and also weighed.

The temperature and pressure in the saturator are held precisely steady during a run and measured accurately. The quantities of water and oxygen are determined by accurate weighing with detailed attention to buoyancy effects and to some small corrections necessitated by the procedure. Typically, in a single run approximately 600 g of oxygen is passed at a uniform rate for a period of several hours. Much additional time is involved in preparing the apparatus, setting the conditions, and carrying out the numerous weighing operations involved.

The value of f_w is calculated from eq 3 in the more explicit form

$$f_w = \frac{m_w/M_w}{m_o/M_o + m_w/M_w}\left[\frac{p}{p_w^o(T)}\right] \quad (9)$$

where M_w and m_w are, respectively, the molecular weight and observed mass of the water and M_o and m_o the corresponding quantities for the oxygen.

Oxygen. The gas used was prepared commercially by the fractional distillation of liquified air and supplied in cylinders at a pressure of approximately 24 MPa. Because of the similarity of the intermolecular forces in oxygen and argon, the latter is by a wide margin the principal impurity in the gas. In air, the quantity of argon expressed as a percentage by volume of the quantity of oxygen is approximately 4.4%. The supplier regarded the oxygen used as containing 0.5−1.0% of argon by volume. No determination of the argon content of the oxygen actually used was made, but it is shown below that the absence of this information does not significantly affect the highly accurate data for B_{ow}, C_{oow}, f_w, and g_w derived from the measurements. In fact, it will be seen from the results that the argon content could not have varied much from 0.4% by volume throughout the work.

Table 1. Experimental Values for the Vapor-Pressure (or Mole-Fraction) Enhancement Factor f_w for Water in Oxygen[a]

p/MPa	t = 25 °C	t = 50 °C	t = 75 °C
2.1580	1.0497	1.0428	
3.5360	1.0843	1.0683	1.0610
6.9850	1.1654	1.1360	1.1175
10.1010	1.2494	1.2002	1.1681
14.0850	1.3525	1.2833	1.2370

[a] Each value is the mean of, on the average, five results.

Results. For temperatures of 25 and 50 °C measurements of f_w were made for five pressures from 2.158 to 14.085 MPa, and for a temperature of 75 °C for four pressures from 3.536 to 14.085 MPa. In calculating f_w from the measurements by means of eq 9, the molecular weights used have been based on $^{12}C = 12$, and that of the oxygen has been the value for the pure gas (31.9988). The implications of the latter choice are considered below. The molecular weight of water is 18.0153. Its saturation vapor pressure has been given by Wexler (1976).

On the average, five runs were made for each set of conditions. A summary of the results is given in Table 1. For purposes of this summary, each individual result was adjusted to correspond accurately to the nominal experimental conditions, and the mean then calculated for each set. The deviations of the individual results may be seen in Figure 1, referred to further below.

Derivation of $B_{ow}(T)$ and $C_{oow}(T)$

To derive data for $B_{ow}(T)$ and $C_{oow}(T)$ from the experimental data for $f_w(T,p)$ using eq 6, we require independent data for $B_{ww}(T)$, $C_{www}(T)$, $C_{oww}(T)$, $\tilde{V}_w^{l,o}(T,p)$, and $x_o^l(T,p)$. Also, the equation of state of oxygen is needed in the calculation of $Z(T,p)$ and hence also $\tilde{V}(T,p)$ for the mixture. The appropriate data for $B_{ww}(T)$, $C_{www}(T)$, and $\tilde{V}_w^{l,o}(T,p)$ are as for water in air (Wylie and Fisher, 1996). For $x_o^l(T,p)$, which is only marginally significant, the temperature dependence of the low-pressure solubility of oxygen in water has been taken from Himmelblau (1960), and the pressure dependence of the solubility from Zoss *et al.* (1954). The generation of data for $C_{oww}(T)$ and the treatment of the data available for the equation of state of oxygen warrant detailed consideration.

Estimation of $C_{oww}(T)$. For water in air the only data available for the corresponding quantity $C_{aww}(T)$ was a theoretical estimate published by Hyland and Mason (1975), which we adopted with a 3σ uncertainty of 200%. For $C_{oww}(T)$ not even an estimate has been given, and so we have used the Hyland and Mason procedure to make our own. This involves the extension to mixtures of Woolley's model (1953) of an imperfect gas as consisting of a perfect gas containing single molecules (monomers), dimers, trimers, etc., and the treatment (to third virial and

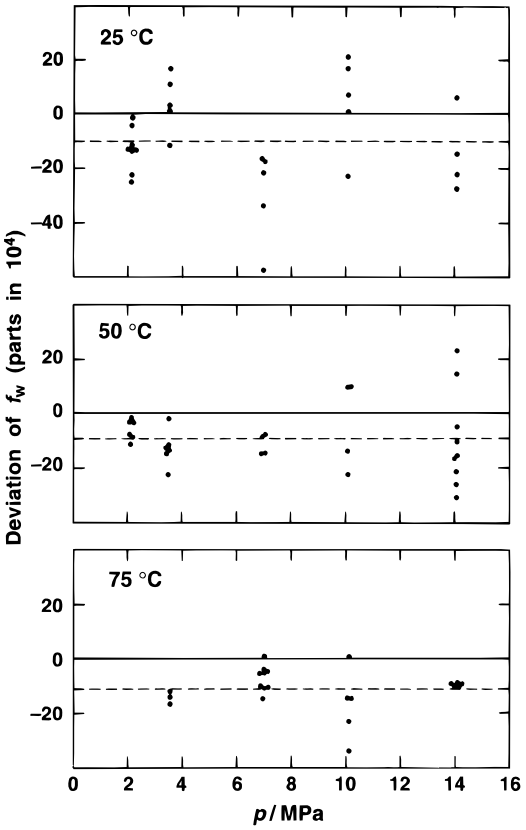

Figure 1. Deviations of the individual experimental values of f_w from the values given by eq 6 with $B_{ow}(T)$ and $C_{oow}(T)$ fitted separately for each temperature (Table 4).

third interaction virial coefficients) of the water−oxygen mixture as consisting of oxygen monomers, water monomers, and water dimers. These species self-interact and mutually interact two by two, except that water monomers do not interact with one another as this would be redundant with the inclusion of the dimers.

Following Hyland and Mason (1975), the required coefficient $C_{oww}(T)$ is given by

$$C_{oww} = -(2/3)B_{ow2}B_{ww} \qquad (10)$$

where w2 denotes the dimer. The experimental quantity B_{ww} is the same in our calculation as in that for water in air. To obtain B_{ow2}, the well depth ϵ and distance parameter σ for the equivalent Lennard-Jones (L-J) (6−12) intermolecular potential (Hirschfelder *et al.*, 1964) are estimated by applying conventional combining rules to the corresponding parameters for oxygen−oxygen interactions and the spherical parts of the water−water interaction and the water−dimer interaction.

We derive the appropriate parameters for the oxygen−oxygen interaction from the experimental data of Michels, Schamp, and de Graaff (1954), finding

$$\epsilon_{oo}/k = 121\ \text{K} \quad \text{and} \quad \sigma_{oo} = 3.39 \times 10^{-10}\ \text{m} \qquad (11)$$

where k is the Boltzmann constant. The corresponding parameters for the spherical parts of the water−water and water−dimer interactions are obtained directly from Hyland and Mason. For the latter interaction we adopt the values derived from viscosity data. We then obtain

$$\epsilon_{ow2}/k = 327\ \text{K} \quad \text{and} \quad \sigma_{ow2} = 3.48 \times 10^{-10}\ \text{m} \qquad (12)$$

from which $B_{ow2}(T)$ can be calculated.

Table 2. Values of the Interaction Virial Coefficient $C_{oww}(T)$ for Water Vapor in Oxygen, Derived Theoretically by the Method of Hyland and Mason (1975)

t/°C	$-10^{-3}C_{oww}(T)$/(cm³/mol)²	t/°C	$-10^{-3}C_{oww}(T)$/(cm³/mol)²
0	225	60	61
10	174	70	52
20	137	80	44
30	110	90	37
40	89	100	32
50	74		

Table 3. Skeletal Table of the Compressibility Factor $Z(T,p)$ Adopted for Pure Oxygen

t/°C	p/MPa = 3	p/MPa = 6	p/MPa = 9	p/MPa = 12	p/MPa = 15
0	0.9723	0.9482	0.9284	0.9139	0.9052
25	0.9817	0.9665	0.9550	0.9475	0.9443
50	0.9885	0.9796	0.9737	0.9710	0.9715
75	0.9933	0.9890	0.9870	0.9877	0.9909
100	0.9969	0.9958	0.9968	0.9998	1.0051

Applying eq 10, we find the values of C_{oww} tabulated for temperatures of 0−100 °C in Table 2. The uncertainties involved are similar to those for water in air, and again we adopt a 3σ value of 200%.

Equation of State of Oxygen. Reliable PVT data for oxygen are sparse for temperatures above 0 °C and the present pressures. For the analysis we must know the compressibility factor $Z = p\tilde{V}/RT$ of oxygen for temperatures of 25, 50, and 75 °C and pressures to approximately 14 MPa. Further, we wish to extend our calculations of g_w and f_w to 0 and 100 °C, and to 15 MPa. The most reliable data, those of Michels *et al.* (1954), are for temperatures of 0, 25, and 50 °C and pressures to 13 MPa (but 12 MPa at 0 °C). We have adopted these, and interpolated and extrapolated them by a special physically-based method. This takes advantage of the close similarity of the equations of state of oxygen and nitrogen and the especially good knowledge which exists of the latter.

Using the principle of corresponding states (Hirschfelder *et al.*, 1964), the data of Michels *et al.* may be correlated with corresponding data taken from the Jacobsen and Stewart collation (1973) of the results of various researchers. By minimizing the rms error of the correlation, the relationship between corresponding temperatures, that between corresponding pressures, and hence that between corresponding molar volumes are found to be

$$T_{N_2} = 0.80438T_{O_2}$$

$$p_{N_2} = 0.64450p_{O_2} \qquad (13)$$

$$\tilde{V}_{N_2} = 1.24807\tilde{V}_{O_2}$$

Over the range of the Michels data, the rms error of the correlation is only 4.0 parts in 10^4. However, the error is largely systematic. Its trend suggests that a modest reduction in the maximum error in using the correlation to extrapolate the Z for oxygen to 100 °C and to 15 MPa is likely to be gained if the resulting Z is multiplied by the factor

$$1 + 6.0 \times 10^{-4}[(p/\text{MPa} - 6.0)^2/36.0 - 1] \qquad (14)$$

Some sample values of the Z which result from the whole procedure are given in Table 3. We estimate that for temperatures from 0 to 50 °C the 3σ uncertainty in this Z arises largely from that in the Michels data and increases in proportion to the pressure to 15 parts in 10^4 at 15 MPa. For higher temperatures, up to 100 °C, we estimate that

Table 4. Values of a, B_{ow}, C_{oow}, and Their 3σ Uncertainties for the Experimental Temperatures

		$10^4 \times$ uncertainty		uncertainty/(cm^3/mol)				uncertainty/(cm^3/mol)^2		
t/°C	10^4a	rand	B_{ow}/(cm^3/mol)	rand	syst	total	C_{oow}/(cm^3/mol)^2	rand	syst	total
25	−10	35	−27.04	1.38	0.45	1.44	1322	270	54	270
50	−9	26	−20.58	1.05	1.02	1.47	1121	230	90	240
75	−11	35	−15.40	1.14	1.95	2.25	1060	230	144	280

the increase is to 20 parts in 10^4 at this pressure. Conservatively, we have taken the uncertainties in Z for different temperatures to be fully correlated.

To obtain Z and $\tilde{V}$ for a mixture of water vapor and oxygen at a particular temperature, a set of virial and pseudovirial coefficients for oxygen up to the sixth (i.e., the coefficient of $\tilde{V}^{-5}$) may be obtained for that temperature from the Z for oxygen and used in eq 5 in the manner and with the justification detailed for water in air (Wylie and Fisher, 1996).

B_{ow} and C_{oow} for the Experimental Temperatures. The analysis closely parallels that for water in air. For a given temperature the changes in the calculated ln f_w for increments in the B_{ow} and C_{oow} substituted in eq 6 are almost proportional to p and p^2, respectively. Thus, when approximate values of those coefficients are substituted and the differences in the calculated values of ln f_w from the experimental values are least-squares-fitted by a quadratic polynomial in p, the coefficients found for p and p^2 give adjustments which should be made to B_{ow} and C_{oow}. Even a single iteration of the procedure is likely to suffice. The constant term obtained in the least-squares fit, which we denote by a, ideally should be zero, but inevitably a small nonzero value is found. This is believed to arise largely from the presence of a small amount of argon in the oxygen for which no allowance has been made in the molecular weight used in eq 9. The deviations of the individual measurements from the final fits for the three temperatures are plotted in Figure 1.

For each experimental temperature, as a mathematical property of the least-squares fitting process, the random uncertainties in the values found for B_{ow} and C_{oow} are highly correlated. Indeed, the correlation coefficient for $-B_{ow}$ and C_{oow} is 0.98, which we round to unity. The random uncertainties in the values found for different experimental temperatures are, of course, uncorrelated. The systematic uncertainties in B_{ow} and C_{oow} are the sums (with due regard to sign) of the uncertainties in eq 6 which are proportional to p and p^2, respectively. The term in C_{oww} can be resolved without significant residue into a term proportional to p and another proportional to p^2, and makes the dominant contributions to these systematic uncertainties. Therefore, the conservative approximation has been made that all the systematic uncertainties are mutually fully correlated (with proper regard to sign). The values found for a, B_{ow}, and C_{oow} and their uncertainties are given in Table 4.

The value of a, which is seen to be approximately the same for each experimental temperature, corresponds to an argon content of the commercial oxygen of 0.4%. That the values derived for B_{ow} and C_{oow} are independent of a means that they are very insensitive to an error in p_w^o which is constant at a constant temperature and hence to a constant error in any of the experimental temperatures. They are also very insensitive to an error in the adopted molecular weight of the oxygen used, to the value of Z_w^o, and to a constant fractional error in the measured pressure.

B_{ow} and C_{oow} for a Range of Temperature. To interpolate and extrapolate $B_{ow}(T)$, we have used a least-squares method to fit an L-J (6−12) potential to the three experimental values of $B_{ow}(T)$ (Table 4). In the notation of Hirschfelder *et al.* (1964) the result is

$$\epsilon/k = 132.99 \text{ K}$$

$$b_o = 59.35 \text{ cm}^3/\text{mol} \qquad (15)$$

If an L-J (6−18) or an L-J (6−24) potential is fitted instead, the resulting $B_{ow}(T)$ is insignificantly different.

The total uncertainty in a value of $B_{ow}(T)$ calculated from eq 15 comprises six components, three of which are uncorrelated random components arising from the random uncertainties in the three fitted values, and three are corresponding systematic components which, conservatively, have been regarded as mutually fully correlated.

Values of B_{ow}, $T(B_{ow}/dT)$, and $T^2(d^2B_{ow}/dT^2)$ calculated from eq 15 are given with their 3σ total uncertainties in Table 5 for temperatures from −100 to +200 °C. A plot of $B_{ow}(T)$ and its uncertainty limits is given in Figure 2 for temperatures from −50 to +150 °C. The deviations of the experimental values (Table 4) from those in Table 5 are only −0.04, +0.06, and −0.07 cm^3/mol at 25, 50, and 75 °C, respectively. It is not clear why these differences, like the corresponding differences for water in air, are so small.

Lacking reliable theoretical guidance as to the shape of the $C_{oow}(T)$ curve, we can do no better than adopt a weighted linear least-squares fit of the three measured values. This gives

$$C_{oow}(T)/(\text{cm}^3/\text{mol})^2 = 1420 - 5.1t/°\text{C} \qquad (16)$$

The total uncertainty in a value of $C_{oow}(T)$ calculated from eq 16 includes three random and three systematic components analogous to those for B_{ow}, but for C_{oow} we have included a fourth (statistically independent) systematic component to allow for our lack of knowledge of the true shape of the curve. This component has been taken to vary smoothly from 100 mL/mol at 0 °C to 40 at 25, 20 at 50, 30 at 75, and 60 at 100.

The relationship of eq 16 to the three experimental values and their 3σ total uncertainties may be seen in

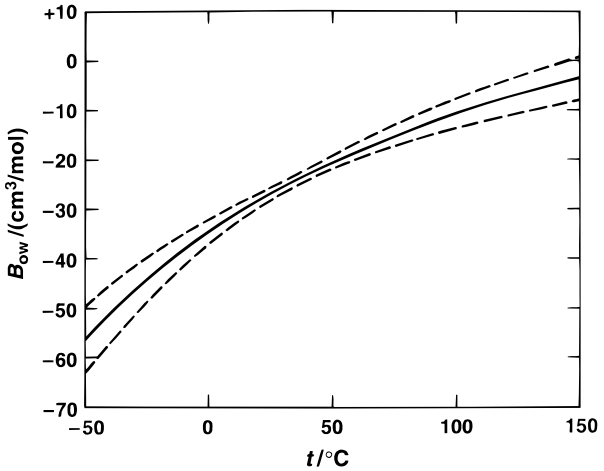

Figure 2. Derived interaction second virial coefficient $B_{ow}(T)$ and its 3σ total-uncertainty limits (broken lines). The deviations of the values derived for the three experimental temperatures (see Tables 4 and 5) are not discernible on this scale.

Table 5. Values and 3σ Uncertainties of B_{ow}, $T(dB_{ow}/dT)$, and $T^2(d^2B_{ow}/dT^2)$ for Temperatures from −100 to +200 °C

t/°C	B_{ow}/(cm^3/mol)	uncertainty/ (cm^3/mol)	$T(dB_{ow}/dT)$/ (cm^3/mol)	uncertainty/ (cm^3/mol)	$T^2(d^2B_{ow}/dT^2)$/ (cm^3/mol)	uncertainty/ (cm^3/mol)
−100	−93.8	13.6	176	32	−432	72
−90	−84.3	11.8	162	30	−395	67
−80	−76.0	10.2	150	28	−363	63
−70	−68.7	8.9	140	27	−335	59
−60	−62.2	7.6	131	25	−312	56
−50	−56.4	6.5	123	24	−291	53
−40	−51.2	5.5	115	23	−273	50
−30	−46.5	4.6	109	21	−256	48
−20	−42.2	3.8	103	20	−242	45
−10	−38.3	3.1	98.1	19.5	−229	43
0	−34.7	2.5	93.4	18.6	−217	42
5	−33.1	2.2	91.2	18.2	−212	41
10	−31.44	1.90	89.0	17.8	−207	40
15	−29.90	1.67	87.0	17.4	−202	39
20	−28.42	1.47	85.1	17.0	−197	38
25	−27.00	1.32	83.2	16.7	−192	37
30	−25.63	1.22	81.4	16.3	−188	37
35	−24.32	1.18	79.7	16.0	−184	36
40	−23.05	1.20	78.0	15.7	−180	35
45	−21.82	1.26	76.4	15.4	−176	35
50	−20.64	1.36	74.9	15.1	−172	34
55	−19.51	1.49	73.4	14.8	−169	33
60	−18.41	1.63	72.0	14.5	−166	33
65	−17.35	1.79	70.6	14.3	−162	32
70	−16.32	1.95	69.2	14.0	−159	32
75	−15.3	2.1	68.0	13.7	−156	31
80	−14.4	2.3	66.7	13.5	−153	31
85	−13.4	2.4	65.5	13.3	−150	30
90	−12.5	2.6	64.3	13.0	−148	30
95	−11.7	2.8	63.2	12.8	−145	29
100	−10.8	2.9	62.1	12.6	−142	29
110	−9.2	3.2	60.0	12.2	−138	28
120	−7.7	3.5	58.1	11.8	−133	27
130	−6.3	3.8	56.2	11.4	−129	26
140	−4.9	4.0	54.5	11.0	−125	25
150	−3.6	4.3	52.8	10.7	−121	25
160	−2.4	4.5	51.2	10.4	−117	24
170	−1.2	4.8	49.8	10.1	−114	23
180	−0.2	5.0	48.3	9.8	−111	23
190	0.9	5.2	47.0	9.5	−108	22
200	1.9	5.4	45.7	9.3	−105	21

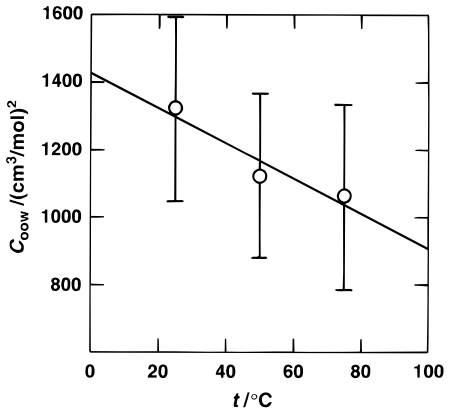

Figure 3. Values of the interaction third virial coefficient $C_{oow}(T)$ derived for the three experimental temperatures, with error bars representing their 3σ total uncertainties, and the straight line resulting from a weighted least-squares fit.

Figure 3. Values calculated from the equation are given with their uncertainties in Table 6 for temperatures of 0−100 °C.

Calculations of g_w and f_w

The vapor concentration enhancement factor $g_w(T,p)$ is given (as ln g_w) by the right-hand side of eq 6 with the first term deleted, and may be calculated by substituting data given above, including those derived for $B_{ow}(T)$ and $C_{oow}(T)$. Every term in the equation for ln g_w approaches zero (and g_w approaches unity) as p is decreased to p^o_w. Therefore, there is no question of including the offset a in the equation. The random and systematic uncertainties in g_w are calculated as the statistical sums of the corresponding uncertainties in the terms, with due regard to the correlations involved. The random uncertainty arises from B_{ow} and C_{oow}, the six contributions from which being correlated as already described. The systematic uncertainty arises very largely from B_{ow}, C_{oow}, and C_{oww}, and as stated above, its components have been regarded as mutually fully correlated (with regard to sign).

Having obtained g_w and its uncertainty, we obtain f_w by multiplying by Z/Z^o_w. To obtain the uncertainty of f_w from that of g_w, we statistically delete the uncertainty of Z, as its effect when g_w is multiplied by Z/Z^o_w roughly cancels with its effect in the analysis which leads to Table 4, but statistically add in the uncertainty in Z^o_w, which has had no earlier effect because the offset a has been taken equal to zero.

Table 6. Values and 3σ Uncertainties of C_{oow} for Temperatures from 0 to 100 °C

t/°C	C_{oow}/ (cm^3/mol)^2	uncertainty/ (cm^3/mol)^2	t/°C	C_{oow}/ (cm^3/mol)^2	uncertainty/ (cm^3/mol)^2
0	1420	410	60	1110	190
10	1370	340	70	1060	230
20	1320	270	80	1010	290
30	1270	220	90	960	350
40	1220	180	100	910	420
50	1170	170			

Table 7. Values of g_w and f_w for Various Temperatures and Pressures[a]

t/°C	p/MPa = 0.1	p/MPa = 1	p/MPa = 2	p/MPa = 5	p/MPa = 10	p/MPa = 15
0	1.00381, 2.2	1.0388, 21	1.0789, 40	1.2058, 87	1.4337, 130	1.6660, 164
	1.00332, 4.6	1.0294, 21	1.0592, 40	1.1530, 87	1.3239, 130	1.5089, 163
20	1.00300, 1.2	1.0310, 11	1.0625, 22	1.1602, 45	1.3283, 58	1.4932, 54
	1.00348, 4.2	1.0250, 12	1.0493, 22	1.1251, 45	1.2595, 57	1.4018, 52
40	1.00231, 0.6	1.0249, 6	1.0502, 11	1.1270, 23	1.2555, 29	1.3786, 27
	1.00423, 4.0	1.0224, 7	1.0428, 12	1.1054, 23	1.2149, 28	1.3294, 23
60	1.00164, 0.4	1.0201, 5	1.0406, 10	1.1024, 21	1.2038, 29	1.2996, 31
	1.00539, 4.0	1.0217, 6	1.0391, 10	1.0922, 20	1.1842, 26	1.2801, 26
80	1.00089, 0.4	1.0162, 7	1.0332, 14	1.0839, 31	1.1662, 44	1.2437, 44
	1.00551, 4.0	1.0228, 8	1.0381, 14	1.0843, 31	1.1643, 42	1.2477, 41
100		1.0129, 10	1.0272, 21	1.0698, 48	1.1388, 77	1.2039, 96
		1.0255, 11	1.0397, 21	1.0813, 48	1.1530, 76	1.2281, 94

[a] Upper values, g_w; lower values, f_w. Uncertainties (3σ) are parts in 10^4.

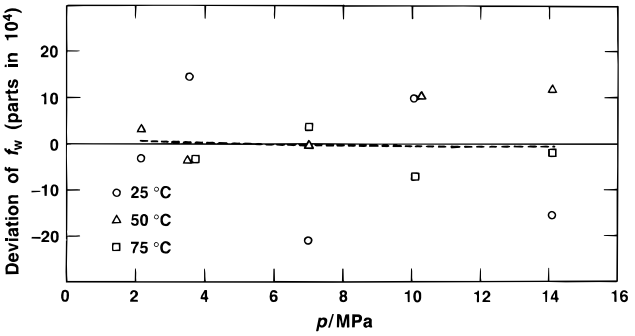

Figure 4. Deviations of the group-average experimental values of f_w (values in Table 1 minus the average of the three values of the offset a in Table 4) from the values given by eq 6 with $B_{ow}(T)$ defined by eq 15 or Table 5 and $C_{oow}(T)$ by eq 16 or Table 6. The broken line represents an unweighted quadratic least-squares fit of the 14 points. The rms deviation of the points from the abscissa is 9.8 parts in 10^4.

Except for this direct effect of an error in Z_w^o on f_w, the insensitivity of B_{ow} and C_{oow} to certain systematic errors, which has been pointed out above, is shared by the calculated values of g_w and f_w.

The group-averaged experimental values of f_w (Table 1), with the mean of the three values of the offset a (Table 4) discounted from each, may be compared with values calculated in this way, in effect from eq 6. The differences of the experimental from the calculated values are plotted in Figure 4. The rms difference is 9.8 parts in 10^4. A least-squares quadratic fit of the differences gives the curve shown as a broken line, which practically coincides with the abscissa axis as it should.

A skeletal tabulation of values of g_w and f_w and their total 3σ uncertainties is given in Table 7 for temperatures from 0 to 100 °C and pressures to 15 MPa.

Literature Cited

Himmelblau, D. M. Solubilities of Inert Gases in H_2O: 0° to near the Critical Point of H_2O. *J. Chem. Eng. Data* **1960**, *5*, 10−15.

Hirschfelder, J. O.; Curtiss, C. F.; Bird, R. B. *Molecular Theory of Gases and Liquids*; Wiley: New York, 1964.

Hyland, R. W.; Mason, E. A. Corrections to Paper Entitled "Third Virial Coefficient for Air-Water Vapour Mixtures". *J. Res. Natl. Bur. Stand. (U.S.)* **1975**, *A79*, 775−776.

Jacobsen, R. T.; Stewart, R. B. Thermodynamic Properties of Nitrogen including Liquid and Vapor Phases from 63 K to 2000 K with Pressures to 10,000 Bar. *J. Phys. Chem. Ref. Data* **1973**, *2*, 757−922.

Michels, A.; Schamp, H. W.; de Graaff, W. Compressibility Isotherms of Oxygen at 0°, 25° and 50 °C and at Pressures up to 135 Atmospheres. *Physica (Amsterdam)* **1954**, *20*, 1209−1214.

Wexler, A. Vapour Pressure Formulation for Water in Range 0 to 100 °C. A Revision. *J. Res. Natl. Bur. Stand. (U.S.)* **1976**, *A80*, 775−785.

Woolley, H. W. The Representation of Gas Properties in Terms of Molecular Clusters. *J. Chem. Phys.* **1953**, *21*, 236−241.

Wylie, R. G.; Fisher, R. S. Molecular Interaction of Water Vapor and Air. *J. Chem. Eng. Data* **1996**, *41*, 133.

Zoss, L. M.; Suciu, S. N.; Sibbitt, W. L. The Solubility of Oxygen in Water. *Trans. ASME* **1954**, *76*, 69−71.

Received for review April 20, 1995. Accepted October 21, 1995.[⊗]

JE950093D

[⊗] Abstract published in *Advance ACS Abstracts*, December 1, 1995.